

COMPACT PROTON INJECTOR AND FIRST ACCELERATOR SYSTEM TEST FOR COMPACT PROTON DIELECTRIC WALL CANCER THERAPY ACCELERATOR*

Y.-J. Chen[#], G. Guethlein, G. Caporaso, S. Sampayan, G. Akana, R. Anaya, D. Anderson, D. Blackfield, J. Carroll, E. Cook, S. Falabella, J. Harris, S. Hawkins, B. Hickman, C. Holmes, S. Nelson, B. Poole, R. Richardson, D. Sanders, J. Stanley, J. Sullivan, L. Wang, J. Watson, LLNL, Livermore, CA, USA
J. Weir, Compact Particle Accelerator Co., Madison, WI, USA
D. Pearson, TomoTherapy, Madison, WI, USA

Abstract

A compact proton accelerator for cancer treatment is being developed by using the high-gradient dielectric insulator wall (DWA) technology [1-4]. We are testing all the essential DWA components, including a compact proton source, on the First Article System Test (FAST). The configuration and progress on the injector and FAST will be presented.

INTRODUCTION

Our goal is to fit the proton machine inside a conventional treatment room. To make the proton DWA accelerator compact requires five essential elements: high gradient insulators (HGI) with high surface breakdown strength, a pulse forming line architecture providing square pulses, fast switches with high bulk breakdown strength, large dielectrics with high dielectric constant and bulk breakdown strength, and a compact proton source capable of delivering sub-ns proton bunches. We are testing these components on FAST, which could be taken apart and rebuilt rapidly to increase system performance by using improved components.

FIRST ARTICLE SYSTEM TEST

FAST is a Blumlein accelerator system consisting of a stack of 1.83-cm high HGI and 7 Blumeins containing SiC photoconductive switches (shown in Figure 1). Coupled directly into the HGI, all Blumeins are fired at the same time when the switches are illuminated with an expanded laser beam simultaneously. While the FR-4 solid dielectric in the Blumeins was anticipated to be the electrical weak point, the switches had bulk breakdown due to structural defects. Our first SiC wafers, from a different supplier, were free of these defects and exhibited bulk breakdown strength close to 250 MV/m. We have obtained new defect free SiC wafers from another source.

FAST was first operated as a diode with a flashboard cathode and a wire mesh at each end of the HGI. The Blumeins impedance is about 40 Ω . Beam loading from either the electron or proton beam is negligible. Hence, the 3-ns output voltage across the HGI rang for several

cycles (see Figure 2). Figure 3 shows that FAST's accelerating field is sensitive to the switches' on-resistance, determined by the driving laser's power, the ability to get laser power into the switches, and the design and impurity properties of the switches. The FAST switches failed around the edges at about 350 MV/m due to the edge enhancement effect of switch packaging in the Blumeins, while the average field stress in the switches was about 30 MV/m, which limited FAST accelerating voltage to about 8 kV.

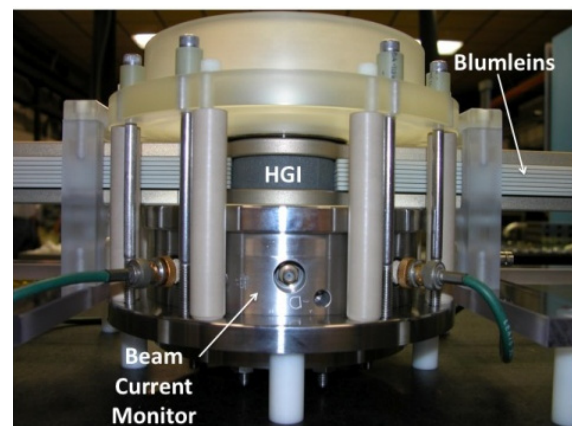


Figure 1: First article system test.

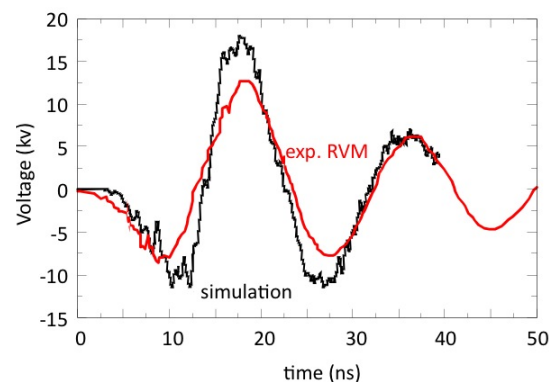


Figure 2: The FAST's accelerating voltage pulse.

*This work was performed under the auspices of the U.S. Department of Energy by University of California, Lawrence Livermore National Laboratory under Contract DE-AC52-07NA27344.

[#]chen6@llnl.gov

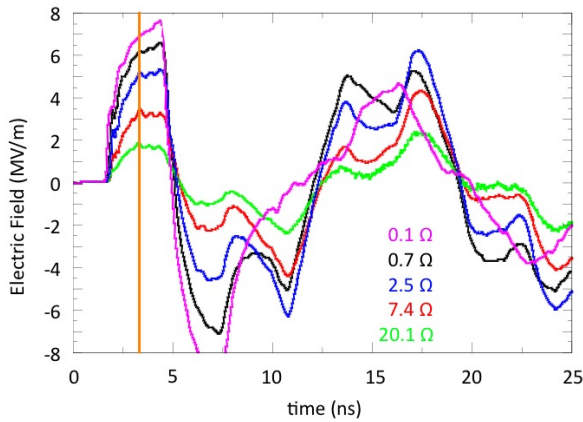


Figure 3: The FAST’s on-axis accelerating field waveform with various SiC on-resistance.

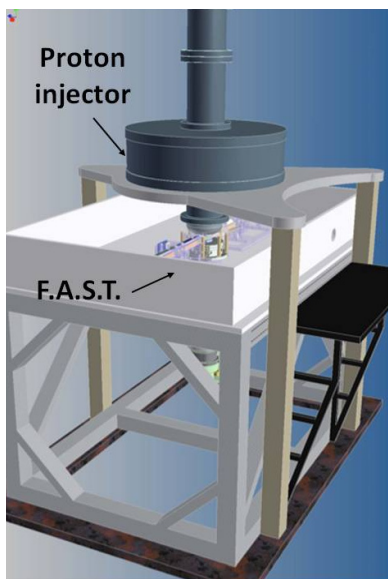


Figure 4: Proton injector and FAST test stand.

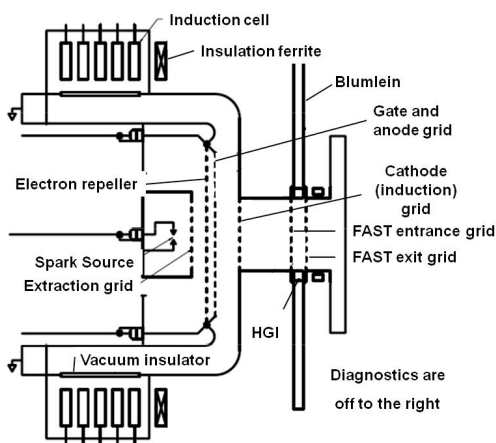


Figure 5: Layout of proton injector and FAST.

INJECTOR TEST STAND

The proton injector is mounted on the top of the FAST (see Figures 4 and 5). The spark source [4] was operated with hydrogen loaded Ti and 4.7 kV, 175 ns, 60 A spark drive. The spark plasma expands for 2.5 cm before the extraction grid. The spark and extraction grid are biased at +600 V. Following that is a grounded electron repelling grid. The gate grid was biased to +3.4 kV, blocking ion transport until the 20 ns FWHM, 10 kV gate pulse arrives. The region between the gate/anode grid and anode grid is a 3-cm A-K gap. An induction system consisting of 5 induction cells with 5 spark gap switched Blumleins provides the A-K gap voltage up to 250 kV, with a 30 ns rise time and no flattop, to ensure proton transit time in FAST shorter than 3 ns so protons would be accelerated while passing through FAST. The 10-keV proton’s transient time through the 250-kV A-K gap is about 7 ns. There is a 2.15-cm drift before FAST’s entrance grid. The DWA accelerator section is terminated with a grid.

ENERGY MODULATION

Since the FAST acceleration voltage range for several cycles, protons would be accelerated or decelerated based on the FAST timing. Calculations of proton energy after FAST with the FAST voltages at 8 kV, 30 kV and 60 kV are given in Figure 6. For each FAST voltage, the proton energies for the timing set to (a) accelerate and (c) decelerate protons, and (b) no FAST pulse are plotted. The horizontal axis is time normalized to the proton transit time through FAST. The multiple values of beam energy at a given time are due to protons’ catching up or slipping along the beam pulse. Energy modulations by the FAST timing for all 3 voltage levels can be easily observed. For example, the modulation introduced by the 8-kV FAST’s timing can be observed with either time resolved or integrated energy diagnostics. Simulations done with a 2-D EM particle-in-cell code, LSP, yields the similar results.

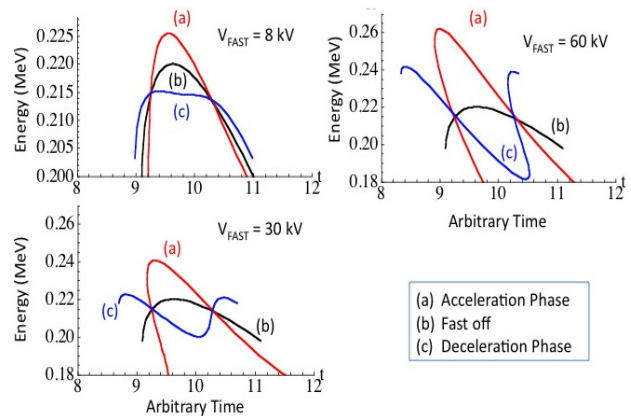


Figure 6: Proton energy after FAST.

DIAGNOSTICS

An ion collector with entrance grid is located 15.7 cm downstream of the DWA exit grid. An 1-mm (2mm) aperture in the ion collector's entrance grid allows passage of ions into a slit collimator (0.25 mm x 1.5 mm with 62 mm separation) at the entrance to the Thomson spectrometer. This choice gives a proton energy resolution of a few keV, with less concern for the mass resolution. Permanent magnets with $B \cdot dl = 18$ kG-cm and a variable electric field deflected the ions. 17.3 cm from the magnet center, a micro-channel plate with phosphor anode was used for ion detection. Images were recorded by a camera with gated intensifier.

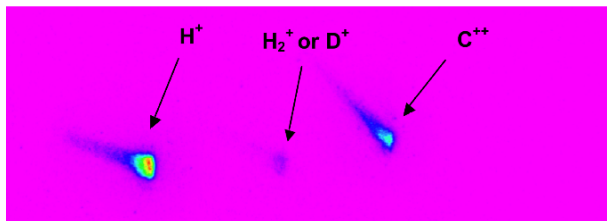


Figure 7: Typical Thomson spectrometer image. Position of undeflected axis is off the right side of the image. Long dimension of slit is vertical in this image. Magnetic deflection is to the left, and electric deflection is upward in the image.

RESULTS

A proton current of a few mA is typically observed on the ion collector. Prior to energizing the DWA, the full mass spectrum was recorded with the Thomson spectrometer. A typical spectrum is shown in Figure 7, with an inductive acceleration of 210 kV. The spectra are consistent with the normalized mass to charge ratios, m/q , being 1, 2, and 6, which are interpreted as H^+ , D^+ , and C^{2+} . Hydrogen, bound atomically to the Ti surface in the spark source, is released during the spark and then ionized. Without a hydrogen gas fill, few molecular ions are expected [6]. The ion signal at $m/q = 2$ is less than 10% of the H^+ signal, but significantly above the 1.2×10^{-4} fraction of naturally occurring deuterium. It is possible due to deuterium contamination of the source Ti, since the hydrogen loading of Ti for this source was performed after the system was used to load deuterium for a D^+ source. Tests upcoming this year will determine if that is the cause of the $m/q = 2$ signal. To minimize the heavier ion impurities, the gate is pulsed early to capture the leading edge of the spark plasma. Acceleration of the C^{2+} ions in the injector and by the FAST is small due to their long transit times across the A-K gap and the FAST DWA structure plus the late arrival time at the FAST. Ions with larger m/q , such as OH^+ and C^+ , are not accelerated as their transit time across the A-K gap is longer than the duration of the induction accelerator pulse, which may explain why they are not observed. In Figure 8, the region of the Thomson spectra proximate to the H^+ is shown, and the effect of energizing FAST is easily observed. The

timing of FAST was set such that proton energies were increased or decreased as shown. The peak energy shift is consistent with the integrated FAST voltage waveform over a proton transit time at this injection energy as is the relative width of the energy spectra for the 3 cases (compare with Figure 6a).

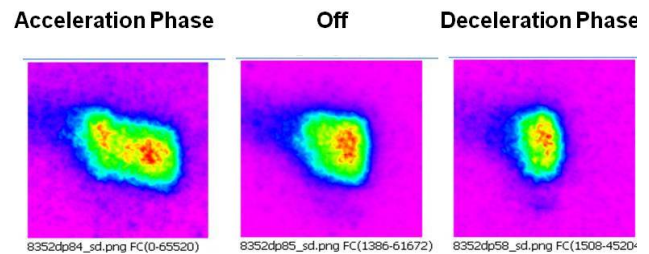


Figure 8: Magnified region around H^+ shows an increase in energy (less deflection) when FAST is energized and phased to accelerate protons.

REFERENCES

- [1] G. Caporaso, et. al., "Compact Accelerator Concept of Proton Therapy", Nucl. Instr. and Meth. in Phys. B 261, p. 777 (2007); www.sciencedirect.com.
- [2] G. Caporaso, et. al., "High Gradient Induction Accelerator", PAC'07, Albuquerque, June 2007, TUYC02, p. 857 (2007); <http://www.JACoW.org>.
- [3] Y.-J. Chen and A. C. Paul, "Compact Proton Accelerator for Cancer Therapy", PAC'07, Albuquerque, June 2007, TUPAS059, p. 1787 (2007); <http://www.JACoW.org>.
- [4] G. Caporaso, et. al., "Status of the Dielectric Wall Accelerator", PAC'09, Vancouver, Canada, May 2009, TH3GAI02, (2009); <http://www.JACoW.org>.
- [5] S. Falabella, et.al., "Characterization of a Surface-Flashover Ion Source with 10-250 ns Pulse Widths", Proc. of the 12th CAARI, March 2009, Vol. 1099, p. 99 (2009).
- [6] E. Cheifetz, U. Adar, and G. Davara, Proc. 17th International Symposium on Discharges and Electrical Insulation in Vacuum, Berkeley, p194 (1996).